JOURNAL OF BACTERIOLOGY, Sept. 1994, p. 5654–5664
0021-9193/94/$04.00+0

Vol. 176, No. 18

Trehalose-6-Phosphate Hydrolase of *Escherichia coli*

MARTINA RIMMELE AND WINFRIED BOOS*

Department of Biology, University of Konstanz, D-78434 Konstanz, Germany

Received 13 May 1994/Accepted 7 July 1994

The disaccharide trehalose acts as an osmoprotectant as well as a carbon source in *Escherichia coli*. At high osmolarity of the growth medium, the cells synthesize large amounts of trehalose internally as an osmoprotectant. However, they can also degrade trehalose as the sole source of carbon under both high- and low-osmolarity growth conditions. The modes of trehalose utilization are different under the two conditions and have to be well regulated (W. Boos, U. Ehmann, H. Forkl, W. Klein, M. Rimmele, and P. Postma, J. Bacteriol. 172:3450–3461, 1990). At low osmolarity, trehalose is transported via a trehalose-specific enzyme II of the phosphotransferase system, encoded by *treB*. The trehalose-6-phosphate formed internally is hydrolyzed to glucose and glucose 6-phosphate by the key enzyme of the system, trehalose-6-phosphate hydrolase, encoded by *treC*. We have cloned *treC*, contained in an operon with *treB* as the promoter-proximal gene. We have overproduced and purified the *treC* gene product and identified it as a protein consisting of a single polypeptide with an apparent molecular weight of 62,000 as determined by sodium dodecyl sulfate-polyacrylamide gel electrophoresis. The enzyme hydrolyzes trehalose-6-phosphate with a K_m of 6 mM and a V_{max} of at least 5.5 μmol of trehalose-6-phosphate hydrolyzed per min per mg of protein. The enzyme also very effectively hydrolyzes *p*-nitrophenyl-α-D-glucopyranoside, but it does not recognize trehalose, sucrose, maltose, isomaltose, or maltodextrins. *treC* was sequenced and found to encode a polypeptide with a calculated molecular weight of 63,781. The amino acid sequence deduced from the DNA sequence shows homology (50% identity) with those of oligo-1,6-glucosidases (sucrase-isomaltases) of *Bacillus* spp. but not with those of other disaccharide phosphate hydrolases. This report corrects our previous view on the function of the *treC* gene product as an amylotrehalase, which was based on the analysis of the metabolic products of trehalose metabolism in whole cells.

The disaccharide trehalose serves as an osmoprotectant in many different organisms. Its two glucose molecules are linked 1-1 α-glycosidically. Thus, the sugar is nonreducing and has the unique quality of maintaining the fluidity of membranes under conditions of dryness and desiccation (16, 17). In *Escherichia coli*, trehalose is synthesized internally as an answer to osmotic stress (23, 45, 48). Among other, more prominent osmoprotectants such as glycine betaine or proline (11, 36), trehalose can contribute up to 20% of the entire capacity for osmotic protection of the cell (21, 32). To synthesize the osmoprotectant trehalose at high osmolarity, UDP-glucose and glucose 6-phosphate are used to form trehalose-6-phosphate, regardless of the carbon source. Trehalose-6-phosphate is subsequently dephosphorylated to give free trehalose. Trehalose-6-phosphate synthase is encoded by *otsA* (osmotic trehalose synthesis), and trehalose-6-phosphate phosphatase is encoded by *otsB*. The two genes are localized at 42 min on the chromosome, *otsB* being the promoter-proximal gene of the operon (21, 23). The operon is induced by high osmolarity, and at least the synthase is activated by potassium (23), which is accumulated in response to osmotic stress (8). Induction of the *ots* operon is also dependent on RpoS, the alternative sigma factor of stationary-phase cells (26).

E. coli can grow on trehalose as the sole source of carbon at low and high osmolarity, when the sugar is synthesized and accumulated internally. This seemingly paradoxical situation of degrading trehalose as a carbon source and synthesizing it as an osmoprotectant at the same time is solved by *E. coli* in an intriguing way. The bacterium has developed two different systems of trehalose metabolism, one for high osmolarity and one for low osmolarity.

Under conditions of high osmolarity, trehalose is hydrolyzed to glucose by a periplasmic trehalase, encoded by *treA*, located at 26 min on the *E. coli* chromosome (7, 24). Glucose is subsequently taken up by the phosphotransferase system (PTS) as glucose 6-phosphate and enters glycolysis. The periplasmic trehalase, TreA, is induced by 250 mM NaCl in the medium but not by trehalose. *treA* mutants can no longer grow on trehalose as the sole source of carbon at high osmolarity (7), but they do grow at low osmolarity (<170 mosM NaCl). Therefore, it is clear that at low osmolarity, a second system for trehalose degradation exists.

As described previously (7, 34), trehalose is transported at low osmolarity via a PTS for trehalose, using specific enzyme $EIICB^{Tre}$ (EII^{Tre}) and the $EIIA^{Glc}$ ($EIII^{Glc}$) of the glucose PTS, delivering trehalose-6-phosphate to the cytoplasm. As we will describe here, the resulting trehalose-6-phosphate is then hydrolyzed to glucose and glucose 6-phosphate by trehalose-6-phosphate hydrolase, the gene product of *treC*. Glucose 6-phosphate and glucose (after being phosphorylated by glucokinase) then enter glycolysis. TreB (EII^{Tre}) and TreC are both induced by trehalose-6-phosphate (28). The genes *treB* and *treC* form an operon, *treB* being the promoter-proximal gene of the operon. They are localized at 96.5 min on the chromosome. The *treB-treC* operon is under cyclic AMP-catabolite gene activation protein regulation and is thus subject to glucose-mediated catabolite repression (7).

Previously (7), we had concluded that the *treC* gene product had the activity of an amylotrehalase, recognizing free trehalose as its substrate. TreC was thought to release one molecule of glucose from trehalose and to transfer the other onto an as-yet-unidentified glucose polymer. The evidence for this

* Corresponding author. Mailing address: Department of Biology, University of Konstanz, D-78434 Konstanz, Germany. Phone: 49 7531 882658. Fax: 49 7531 883356.

TABLE 1. Bacterial strains and plasmids

Strain, plasmid, or phage	Known genotype	Source or reference(s)
BL21 (DE3)	F⁻ *hsdS gal met* r⁻ m⁻ λ_{lys} *placI*^{q}-*lacI*/*placUV5* T7 gene 1	47
CB17	UE26 *treA*::Tn*10*	19
ECL116	F⁻ *endA hsdR* Δ(*argF-lac*)*U169 thi*	15
HB290	MC4100 *minA minB rpsL mgl*	25
HF18	BL21 *tsx*::Tn*10*	H. Fsihi
KRIM4	UE15 *treB*	7
MC4100	F⁻ *araD* Δ(*argF-lac*)*U169 rpsL150 relA1 deoC1 flbB5301 deoC1 ptsF25 rbsR*	14
UE14	MC4100 *treA*::Tn*10*	7
UE15	UE14 Tet^s derivative	7
UE26 (ZSC112L)	F⁻ *ptsG2 ptsM1 glk7 rpsL150*	18
UE49	UE14 φ[(*treC-lacZ*⁺)*1*]λ*plac*Mu55	7
pBR322	High-copy-number vector	5
pHSG575	Low-copy-number vector	51
pPD1	pHSG575 with cloned T7 promoter of pT7-5	20
pT7-5	T7 expression system vector	50
M13mp18 and M13mp19	Sequencing phages	39, 55

scheme was based on experiments with whole cells and cell extracts. After the purification of TreC to homogeneity as reported in this publication, we were unable to demonstrate hydrolysis of free trehalose, even in the presence of purified sugar polymers of *E. coli* cells or in the presence of cellular extract expected to contain the putative polysaccharide acceptor for amylotrehalase. Instead, we could demonstrate the ability of the enzyme to hydrolyze trehalose-6-phosphate, thus identifying the enzyme as trehalose-6-phosphate hydrolase.

MATERIALS AND METHODS

Media and growth conditions. Cells were grown at 37°C in minimal medium A (MMA) (42) or in TB medium (42) supplemented with 10 mM $MgSO_4$. As a carbon source in MMA, we used 0.4% glycerol or 0.2% other carbon sources (trehalose, galactose, maltose, or glucose 6-phosphate). Sugars and sugar phosphates were obtained from Sigma. Bacterial strains are derivatives of *E. coli* K-12 and are listed in Table 1. They were constructed by P1 *vir*-mediated transduction (38). The Tn*10* insertions were removed by the method of Bochner et al. (4).

Transport of trehalose. Transport of trehalose was measured as previously described (7), using 45 nM [^{14}C]trehalose (10).

Cloning of *treC* and construction of plasmids (see Fig. 1). Standard DNA methods were used (42). Chromosomal DNA of strain ECL116 (15), partially digested with *Sau*3A and ligated into the *Bam*HI site of pBR322, was used to transform strain UE49, which was then selected for growth on trehalose. Plasmid pUE1 was isolated in this way. A 2.8-kb *Eco*RI-*Cla*I fragment was subcloned into pBR322 that had been digested with *Eco*RI and *Cla*I, yielding pRIM1. Digestion of pRIM1 with *Sca*I and religation resulted in the loss of a 0.7-kb fragment, yielding plasmid pRIM2. pRIM1 was treated with *Eco*RI and *Xmn*I, and the resulting 2.3-kb insert fragment was ligated into pBR322 that had been digested with *Eco*RI and *Eco*RV. This plasmid was called pRIM5. In order to subclone *treB* and *treC* together, we digested pUE1 with *Pst*I. The 6.5-kb *Pst*I fragment was cloned into the *Pst*I site of the low-copy-number vector pHSG575, resulting in pRIM11. The *Pst*I insert of pRIM11 was cloned into the *Pst*I site of pPD1 (20), resulting in pRIM12. The vector pPD1 is a pHSG575 derivative containing the T7 promoter in front of the multiple cloning site.

Expression of TreC in the minicell system. The plasmids pUE1, pRIM1, pRIM2, pRIM5, and, as a control, pBR322 were transformed into strain HB290. Minicells were prepared and the proteins were labeled essentially as described previously (41, 42). Minicells containing 25 μg of protein were resuspended in 0.5 ml of MMA with 0.4% glucose and all amino acids except methionine (0.25 mM each). A 10-μCi amount of [^{35}S]methionine (Amersham International, Bucks, United Kingdom) was added, and the suspension was incubated for 30 min at 37°C. The incorporation of labeled methionine was stopped by the addition of 50 μl of 3 mM methionine, and incubation was continued at 37°C for 5 min. The minicells were harvested, washed in 1 ml of TNE buffer (50 mM Tris-HCl [pH 7.5], 10 mM NaCl, 1 mM EDTA), and resuspended in 25 μl of sodium dodecyl sulfate-polyacrylamide gel electrophoresis (SDS-PAGE) sample buffer. After being heated for 20 min at 50°C, the samples were separated by SDS–12.5% PAGE (29) and autoradiographed.

Cell extracts. Extracts were made from cells grown in TB medium or MMA. A 200-ml overnight culture was washed twice in 10 mM Tris-HCl (pH 7.2)–0.1% β-mercaptoethanol and resuspended in 2 ml of the same buffer. The cells were ruptured in a French pressure cell at 20,000 to 25,000 lb/in^2. The crude extract was centrifuged for 30 min at 4°C at 27,000 × *g*. The supernatant was dialyzed and the protein concentration was determined by the method of Bradford (9), using the protein assay medium of Bio-Rad (Pierce).

Analysis of sugars by TLC. For thin-layer chromatography (TLC), we used precoated TLC plates (Silica 60; Merck). To 10 to 50 μl of cell extracts or purified TreC in 10 mM Tris-HCl (pH 7.0), 10 mM (final concentration) trehalose or trehalose-6-phosphate was added. The solutions were incubated for 1 h at 37°C, and 10 μl was spotted onto a TLC plate and dried. When appropriate and as indicated in Fig. 4, calf intestine alkaline phosphatase (5 U; Boehringer Mannheim) was added and the incubation was continued for 1 h. The reaction mixtures to which alkaline phosphatase had been added were treated with 5 mg of ion-exchange resin (Serdolit MB; Serva) and centrifuged, and the supernatant was spotted onto TLC plates. As controls, 10 μl each of 10 mM glucose, trehalose, glucose 6-phosphate, and trehalose-6-phosphate was spotted. The TLC plates were developed in 1-butanol–ethanol–water (5:3:2), air dried, and sprayed with 20% H_2SO_4. The sugar spots were made visible by charring (100°C).

Determination of the amount of glucose excreted by strain CB17. Strain CB17 was grown overnight in MMA with glycerol and trehalose as the carbon sources. The cells were concentrated to an optical density at 578 nm of 40, and 10 mM trehalose was added. At intervals, 20-μl samples of the cell suspension were centrifuged, and glucose in the supernatant was determined by using glucose oxidase (2) with the glucose oxidase-peroxidase kit of Merck.

TreC assay with PNG as the substrate. A 5- to 20-μl volume of dialyzed cell extracts or purified TreC was added to 0.5 ml of MMA alone or to MMA containing in addition different concentrations of NaCl. A 200-μl amount of *p*-nitrophenyl-α-D-glucopyranoside (PNG) (4 mg/ml in H_2O) was added to start the assay. As soon as the yellow color of *para*-nitrophenol started to appear, the reaction was stopped by the addition of 1 ml 1 M Na_2CO_3. The samples were centrifuged, and the A_{420} of the supernatant was measured. The specific activity of trehalose-6-phosphate hydrolase is given in micromoles of

PNG hydrolyzed per minute and milligram of protein (units per milligram of protein). This assay (in the absence of NaCl) was used throughout this work as a standard. It should be noted that the activity of the enzyme (units per milligram of protein) in this assay is 16-fold lower than in the coupled assay using the natural substrate trehalose-6-phosphate as described below.

Coupled trehalose-6-phosphate hydrolase–glucose 6-phosphate dehydrogenase test. Glucose 6-phosphate produced by TreC-mediated hydrolysis of trehalose-6-phosphate was oxidized to 6-phospho-D-glucono-δ-lactone by glucose 6-phosphate dehydrogenase, thereby reducing $NADP^+$ to NADPH plus H^+. The assay was set up in such a way that the rate of NADPH formation was linear with the amount of TreC and was not limited by substrate or by glucose 6-phosphate dehydrogenase. The increase in A_{340} was measured over time. To 900 μl of 50 mM Tris-HCl (pH 7.5), 0.5 to 50 mM trehalose-6-phosphate, 0.3 mM $NADP^+$ (Boehringer Mannheim), and 10 mM $MgSO_4$ (all final concentrations) were added. Water was added to a final volume of 1 ml. The reaction was started with the addition of dialyzed cell extract (20 μl of a 0.2-mg/ml solution) or pure TreC (5 μl of a 0.4-mg/ml solution) together with glucose 6-phosphate dehydrogenase from Sigma (5 μl of a 0.4-mg/ml solution in H_2O). The reaction was monitored spectrophotometrically over time at 340 nm and room temperature with a Gilford photometer.

Sequencing of *treC* and sequencing strategy. The *treC* sequence was determined by the dideoxy chain termination method of Sanger et al. (43), as modified by Biggin et al. (3). We used universal *lac* primers (United States Biochemicals, Cleveland, Ohio) as well as customized primers (Gesellschaft für angewandte Biotechnologie mbH, Ebersberg, Germany) (MWG) and the Sequenase kit version 2.0 (U.S. Biochemicals). [^{35}S]dATP was purchased from Amersham International. The 2.8-kb *Eco*RI-*Cla*I fragment of plasmid pUE1 containing *treC* (Fig. 1) was cloned into the *Eco*RI-*Acc*I site of the M13 derivatives M13mp18 and M13mp19 (Table 1), yielding M13wk5 and M13wk4, respectively. First we used the universal *lac* primer (17-mer) provided by the sequencing kit for sequencing the insert of M13wk4 and M13wk5. We used the primers indicated in Fig. 5 as customized primers: primers 3 (5′ CGA ACT GGT GAC GCA GG 3′, at position 2124), 4 (5′ GTA CCG CTG GAT TCT CC 3′, at position 2406), 4a (5′ TCA GAT TCA CCA CAT CC 3′, at position 2485), 5 (5′ GAG AAT GAT ACG AAT CC 3′, at position 2169), and 6 (5′ CAT TAC GTT ATT CCT GC 3′, at position 1875). Primer 3 contains the sequence shown in Fig. 5. Primers 4 to 6 are complementary to the sequence shown in Fig. 5. Sequence homologies were found by queries to the latest release of all available databases, using BLAST server at National Center for Biotechnology (NCBI), Bethesda, MD. (1).

Protein homology comparisons were done with the ClustalV program (27).

Purification of TreC. To overexpress TreC for purification, the T7 system of Studier and Moffat (47) was used. Strain HF18 containing plasmid pRIM12, encoding *treC* under the control of the T7 promoter, was grown overnight at 37°C in 4 liters of TB medium containing 0.4% glycerol, chloramphenicol (25 μg/ml), and tetracycline (20 μg/ml). A 2 mM final concentration of isopropyl-β-D-thiogalactopyranoside (IPTG) was added to induce the T7 RNA polymerase encoded chromosomally by the strain, and the culture was incubated further for 40 min. The following procedures were all performed at 4°C. The culture was centrifuged for 15 min at 4,200 × *g*. The pellet was resuspended in 30 ml of 10 mM Tris-HCl (pH 7.5)–1 mM dithiothreitol (DTT). This suspension was ruptured in a French pressure cell at 20,000 lb/in^2. A 10-mg amount of the protease inhibitor phenylmethylsulfonyl fluoride (PMSF) and 100 μg of DNase (bovine grade II; from Boehringer) per ml were added. The suspension was centrifuged for 1 h at 36,900 × *g*. The supernatant (30 ml) was precipitated with 40% ammonium sulfate and centrifuged for 20 min at 27,200 × *g*. The supernatant was precipitated with 100% ammonium sulfate. The resulting pellet was resuspended for 2 h in 10 ml of a 60% ammonium sulfate solution and then centrifuged for 20 min at 27,200 × *g*. The pellet was resuspended in 10 ml of 100 mM Tris-HCl (pH 7.5)–1 mM DTT and dialyzed overnight against 2 liters of 10 mM Tris-HCl (pH 7.5)–1 mM DTT–2 g of PMSF per liter. All the following Tris buffers contained 1 mM DTT and 2 mg of PMSF per ml.

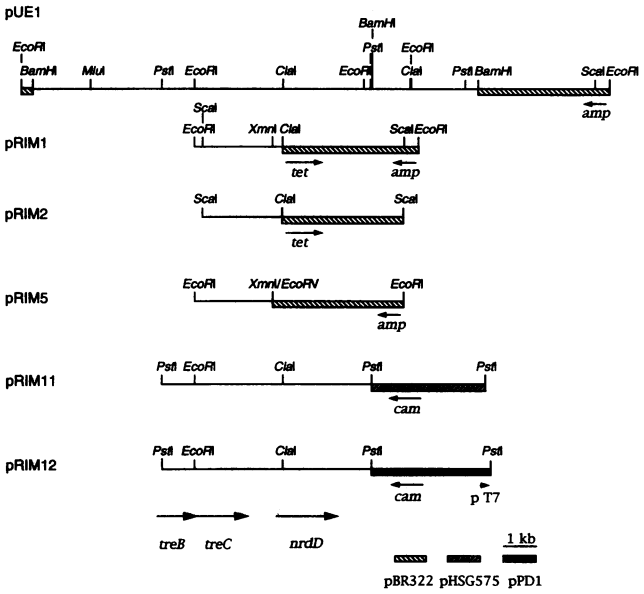

FIG. 1. Plasmids used. The location and direction of the T7 promoter in pRIM12 (p T7) are shown. The extension, location, and direction of *treB*, *treC*, and *nrdD* in the plasmids are indicated below pRIM12. Only the relevant sites are shown in each plasmid.

The dialyzed protein solution was loaded onto an anion-exchange DEAE-Sepharose CL6B column (2.5 [inner diameter] by 9.7 cm) that was equilibrated with 20 mM Tris-HCl (pH 7.5) and washed with 30 ml of the same buffer. The flow rate was 24 ml/h. The column was eluted with 200 ml of a linear 0 to 500 mM NaCl gradient in 20 mM Tris-HCl, pH 7.5. The protein eluted at 250 mM NaCl. Samples containing TreC activity were pooled and precipitated with 100% ammonium sulfate. The pellet was resuspended in 1.5 ml of 100 mM Tris-HCl, pH 7.5. Molecular-sieve chromatography through Sephacryl S200 (1.5 [inner diameter] by 90 cm) equilibrated with 50 mM Tris-HCl (pH 7.5) followed. The flow rate was 8 ml/h. The TreC-containing samples were pooled and chromatographed in 2-ml aliquots on an anion-exchange fast protein liquid chromatography (FPLC) column (MonoQ) equilibrated with 50 mM Tris-HCl, pH 7.5. After being loaded, the column was subjected to a wash with 7.5 ml of the same buffer followed by elution with 40 ml of a linear 0 to 500 mM NaCl gradient in 50 mM Tris-HCl, pH 7.5. The protein eluted again at 250 mM NaCl. The TreC-containing samples were pooled, dialyzed against 50 mM Tris-HCl (pH 7.5), and kept frozen in aliquots at −20°C. Enzymatic activity of the protein

TABLE 2. Specific activity of trehalose-6-phosphate hydrolase in different extracts with the substrate PNG

Strain extract or purified protein	Induction[a]	Addition of NaCl to assay (mM)[b]	U/mg of protein (10^{-3} U/mg of protein)[c]
UE14	−	−	0.8
	+	−	50
	−	+ (300)	2.5
	−[d]	−	0.4
	+	+ (300)	95
UE49			
Alone	−	−	<0.03
With pUE1	−	−	0.3
	+	−	5
With pRIM1	−	−	2.8
	+	−	3.5
With pRIM11	−	−	155
	+	−	157
CB17	−	−	0.75
	−/+	−	51
Purified TreC		−	705
		+ (300)	1,202
		+ (500)	1,674

[a] Uninduced (−) strains were grown in MMA with glycerol. Induction (+) was done by growth in MMA with trehalose. CB17 induction was performed by adding 0.2% trehalose to the glycerol medium (−/+).

[b] Where indicated, NaCl was added to the assay prior to the addition of the substrate PNG.

[c] The activity of TreC is given in units (micromoles of PNG hydrolyzed per minute) per milligram of protein (10^{-3}). Values represent the average of three measurements that did not vary by more than 5%.

[d] This strain was grown in the presence of additional 300 mM NaCl.

samples after each step was followed by PNG assay, Bradford protein determination (9), and SDS-PAGE.

Nucleotide sequence accession number. The nucleotide sequence reported in this paper has been submitted to GenBank under accession number U06195. The protein sequence has been submitted to the Swissprot data bank under accession number P28904.

RESULTS

Cloning of *treC*, encoding trehalose-6-phosphate hydrolase. *treC* was cloned by transforming the Tre$^-$ strain UE49 (*treA*::Tn*10* *treC-lacZ*) with a gene bank of partially digested *Sau*3A chromosomal *E. coli* (Tre$^+$ strain ECL116 [15]) DNA fragments ligated into the *Bam*HI site of pBR322 and selecting for growth on trehalose. Plasmid pUE1 (Fig. 1) complemented the growth defect of UE49 on trehalose and also the Tre$^-$ phenotype of strain KRIM4 (*treA treB*), which is defective in trehalose transport. Thus, pUE1 carries *treB* as well as *treC*. Plasmids containing smaller chromosomal inserts were obtained from pUE1 by subcloning as indicated in Fig. 1. Plasmids pRIM1 and pRIM5, when transformed into strain UE49, yielded only Tre$^+$ clones after a mutational event, indicating, as will become clear later, the lack of an appropriate promoter for *treC*. Neither plasmid complemented KRIM4, indicating the absence of *treB*. Plasmid pRIM2 did not complement the *treC* mutation in strain UE49 and did not show the 62-kDa protein band corresponding to TreC in minicell experiments (data not shown). Plasmid pRIM11, in which the 6.5-kb *Pst*I fragment of pUE1 was cloned into the low-copy-number plasmid pHSG575, complemented the *treC* as well as the *treB* mutation. As shown in Table 2, the presence

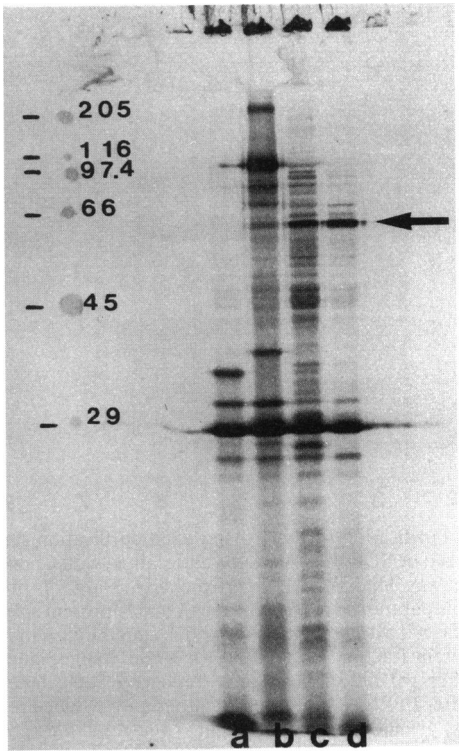

FIG. 2. Expression of plasmid-encoded genes. Plasmids were transformed into strain HB290 and minicells were prepared. Plasmid-encoded proteins were labeled with [^{35}S]methionine and analyzed by SDS–12.5% PAGE. The autoradiogram shows the following plasmids: lane a, pBR322; lane b, pUE1; lane c, pRIM1; lane d, pRIM5. The molecular mass standard (in kilodaltons) is indicated on the left. The arrow points to TreC, a protein of 62 kDa.

of pUE1 in strain UE49 caused trehalose-inducible synthesis of trehalose-6-phosphate hydrolase activity while pRIM1 resulted in a low but constitutive level of enzyme activity. In contrast, pRIM11 expressed high and constitutive levels of the enzyme (Table 2) as well as high levels of transport activity (data not shown). Apparently, pUE1 carried not only the intact *treB-treC* region but also its regulatory elements, while in pRIM11 *treB* and *treC* were under noncognate promoter control. Plasmid pRIM12 contained the insert of pRIM11 under T7 promoter control. Since only one orientation of the insert in pRIM12 (the one shown in Fig. 1) gave T7 promoter-dependent expression of TreC, it is clear that the direction of transcription of *treC* is from left to right, as indicated in Fig. 1.

Expression of *treC* in minicells. The plasmids pUE1, pRIM1, and pRIM5 were transformed into the minicell-producing strain HB290, and the plasmid-encoded proteins were labeled with [^{35}S]methionine, separated by SDS-PAGE, and subjected to autoradiography. The results are shown in Fig. 2. All plasmids encoded a protein with a molecular weight of 62,000. Besides the vector-encoded proteins, this protein was the only one seen in pRIM5. The insert in pRIM5 has a 2.5-kb coding capacity, just 1 kb more than necessary to encode a protein with a molecular weight of 62,000. Since the molecular weight of the purified TreC protein in fact has a molecular weight of 62,000 (Fig. 3), it is obvious that the protein observed in the minicell experiment is encoded by *treC*.

PNG is a substrate of trehalose-6-phosphate hydrolase. We screened the ability of purified TreC protein to hydrolyze

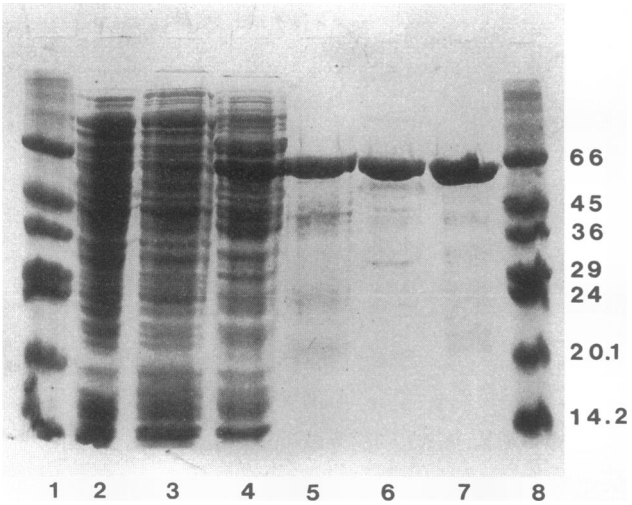

FIG. 3. Purification of TreC. After each purification step, samples were analyzed by SDS–12.5% PAGE and stained with Coomassie blue. Each lane was loaded with approximately 5 μg of protein. The following preparations are shown: lanes 1 and 8, protein size standards; lane 2, crude cell extract; lane 3, 40 to 60% ammonium sulfate fraction; lane 4, protein fraction after DEAE anion exchange; lane 5, protein fraction after gel filtration through Sephacryl S200; lanes 6 and 7, fractions after FPLC (MonoQ) chromatography. Molecular masses (in kilodaltons) are indicated on the right.

trehalose in the presence of maltodextrins of various lengths as well as other polysaccharides extracted from large numbers of cells. We did not observe hydrolysis of trehalose, nor did we observe hydrolysis of maltodextrins of various lengths or of isomaltose or sucrose. Instead, we found that PNG was effectively hydrolyzed by the enzyme to glucose and *p*-nitrophenol. This reaction was rather specific. PNG was not hydrolyzed in extracts lacking TreC, nor was it hydrolyzed by the periplasmic trehalase (6) or by any of the maltodextrin-degrading enzymes, such as amylomaltase (40, 54), amylase (22), or maltodextrin glucosidase (35, 42). The hydrolysis of PNG in 130 mM potassium phosphate (pH 7.0) with 13 mM PNG (which is above the saturating concentration) as a substrate was used to spectrophotometrically assay for TreC activity following the release of *p*-nitrophenol. The data for the specific activity of TreC in various bacterial extracts after growth in the presence and absence of trehalose, as shown in Table 2, were obtained with this assay. We noticed, and this is also shown in Table 2, that the addition of 200 to 500 mM NaCl to the standard assay resulted in an increase of activity. Using the PNG assay, we found that wild-type cells (UE14) were induced by trehalose by a factor of 60. The *treC*::*lacZ* mutant (UE49) essentially lacked any hydrolyzing activity. Cell extracts of UE49 harboring plasmid pUE1 contained trehalose-inducible TreC activity but, surprisingly, to a lesser extent than the wild-type strain UE14 in the absence of any plasmid.

Strains KRIM4 (*treA treB*), CB17 (*treA*::Tn*10 ptsM ptsG glk*), and RIM31 (*treA*::Tn*10 galU*) do not grow, or grow only very slowly, on trehalose. To investigate whether this might be due to a deficiency in TreC activity, we tested different extracts of these strains. The uninduced extracts of the strains were all the same as the uninduced wild-type extract in their TreC activity (data shown only for CB17 in Table 2). Except for the *treB* strain KRIM4, the cells are inducible in their TreC activity when grown in the presence of trehalose. Therefore, a lack of *treC* inducibility or TreC activity is not the reason for their defect in trehalose metabolism.

TABLE 3. Purification procedure for TreC[a]

Purification step product	Amt of protein (mg)	Sp act (μmol/min · mg of protein)	Yield (%)	Fold purification
HF18 pRIM12 French press extract	420	0.22	100	1
40–60% NH_3SO_4 fraction	292	0.23	71	1
DEAE fraction	117.6	0.35	43.8	1.6
Sephacryl S200 fraction	45	0.62	30	2.8
FPLC MonoQ fraction	13	0.70	10.4	3.7

[a] The samples of the different purification steps were tested in the PNG assay to determine micromoles of PNG hydrolyzed per minute per milligram of protein. Values represent the average of three measurements that did not vary by more than 5%.

Purification of trehalose-6-phosphate hydrolase, the *treC* gene product. *treC* was overexpressed under control of the T7 promoter in strain HF18. Purification was achieved by ammonium sulfate precipitation (40 to 60% saturation), DEAE-Sepharose ion-exchange chromatography, molecular-sieve chromatography through Sephacryl S200, and finally ion-exchange chromatography through an FPLC MonoQ column.

Figure 3 and Table 3 show the yield and degree of the purification in the different steps as analyzed by SDS-PAGE and the enzymatic assay with PNG. The protein was essentially pure after the MonoQ FPLC step. From the elution profile of the enzyme in the MonoQ column, it was clear that the molecular weight of the native protein was the same as that of the denatured polypeptide as determined by SDS-PAGE. We obtained 13 mg of trehalose-6-phosphate hydrolase from 4 liters of IPTG-induced cells harvested at an optical density at 578 nm of 2.5. The surprisingly low degree of purification (Fig. 3; Table 3) is likely due to a considerable inactivation of the protein during purification.

The TreC protein hydrolyzes trehalose-6-phosphate. Cell extracts of strains expressing TreC, as well as the pure enzyme, recognize not trehalose but trehalose-6-phosphate as a substrate. Figure 4 shows the analysis by TLC of trehalose and trehalose-6-phosphate after incubation with cell extracts containing TreC or with pure TreC protein. As can be seen in Fig. 4, trehalose-6-phosphate is hydrolyzed to glucose and glucose 6-phosphate (lanes 7 and 9). Glucose 6-phosphate was identified by the addition of alkaline phosphatase to the heat-inactivated incubation mixture with TreC (lane 12), in which glucose was the major product of hydrolysis. The other compound was trehalose, which was formed by the action of alkaline phosphatase on the remaining trehalose-6-phosphate. Neither glucose nor another product is formed when trehalose is added to the pure enzyme (lane 6). On the other hand, cell extracts but not pure TreC form small amounts of glucose from trehalose, indicating the presence of a so-far-unidentified cytoplasmic trehalase that is different from the periplasmic trehalase and from the TreC protein (7, 34). Its activity can also be seen in UE49 extracts. All the strains from which these extracts were obtained are *treA*, thus lacking periplasmic trehalase.

What can also be seen in Fig. 4 is that when trehalose-6-phosphate is incubated with cell extracts (but not with purified TreC protein), there is always, besides the formation of glucose, the formation of trehalose (lanes 9 and 11). The formation of trehalose is most likely due to the activity of trehalose-6-phosphate phosphatase, the *otsB* gene product of the high-osmolarity system, which is still synthesized to some extent at low osmolarity, particularly when the cells have been grown to stationary phase (26). An extract containing large

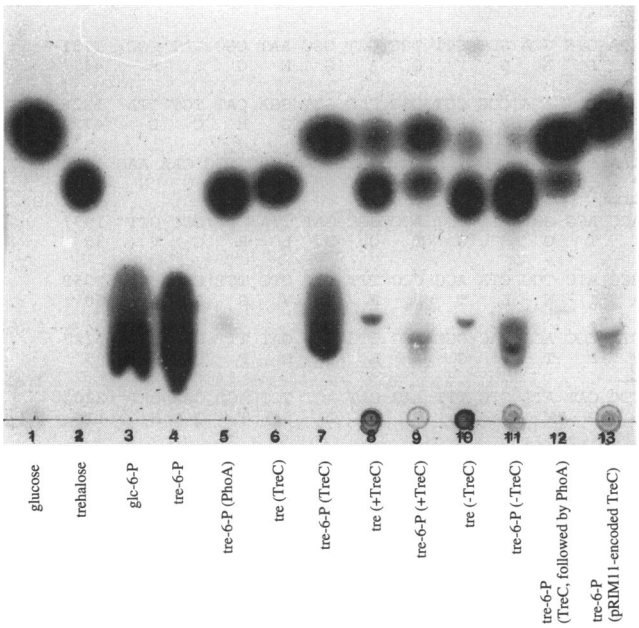

FIG. 4. TLC analysis of trehalose-6-phosphate (tre-6-P) and trehalose (tre) after incubation with TreC. tre-6-P or tre (10 mM each) in 10 mM Tris-HCl (pH 7.0) was incubated for 1 h at 37°C with TreC-containing extracts (+TreC), with purified TreC (TreC), or with extracts of strain UE49 lacking TreC (−TreC). Alkaline phosphatase (PhoA) (5 U) was added as indicated. Lanes 1 to 4, controls (10 μl of a 10 mM solution each). All extracts contained significant amounts of OtsB, hydrolizing tre-6-P to tre (lanes 9 and 11). They also contained small amounts of a trehalase activity of unknown origin, unrelated to TreA or TreC (lanes 8 and 10). A 10-μl sample of each incubation mixture was spotted onto a TLC plate, dried, developed, and visualized by charring.

amounts of trehalose-6-phosphate hydrolase (lane 13) shows no trehalose when incubated with trehalose-6-phosphate, since the substrate is hydrolyzed by TreC before its dephosphorylation by OtsB. To confirm that the product of TreC activity, besides glucose, is glucose 6-phosphate, we used an enzymatic assay that couples the TreC-mediated formation of glucose 6-phosphate from trehalose-6-phosphate with glucose 6-phosphate dehydrogenase. The rate of formation of NADPH upon the addition of the two enzymes to trehalose-6-phosphate and $NADP^+$ was monitored spectrophotometrically. With this test, the K_m and the V_{max} of the enzyme for trehalose-6-phosphate were determined to be 6 mM and 5.5 μmol/min/mg of protein, respectively. The V_{max} is certainly an underestimation of the fully active enzyme, since we had noticed that the enzyme lost activity during purification. When the crude extracts of trehalose-induced cells of UE14 were tested at a 10 mM substrate concentration, a rate of 0.8 μmol/min/mg of protein was obtained.

Determination of the DNA sequence of *treC* and sequence homologies. The *Eco*RI-*Cla*I fragment of pUE1 that is also present in pRIM1 was cloned into M13mp18 and M13mp19 and sequenced by using the universal *lacZ* primer as well as customized primers along the sequence. The sequence of *treC* together with the deduced amino acid sequence is shown in Fig. 5. We had sequenced 791 bp beginning from the *Eco*RI site of the M13 clones and 200 bp beginning from the *Cla*I site (not shown in Fig. 5) when we found that the 3′ end of the *treC* sequence was identical to an incomplete open reading frame reported by Sun et al. (49). Those authors recently published the DNA sequence of the *nrdD* gene, encoding an anaerobic ribonucleotide reductase. Upstream of the *nrdD* sequence, they had found and partly sequenced the 3′ portion of an open reading frame whose deduced amino acid sequence was homologous to an oligo-1,6-glucosidase (53) of *Bacillus cereus*. It became clear that the 3′ end of the *Eco*RI-*Cla*I fragment was identical with the 5′ end of the *nrdD* gene as well as with the 3′ portion of the open reading frame as reported by Sun et al. (49). The sequence already published by Sun et al. is marked in Fig. 5. The *treC* gene starts with the ATG at position 1873 of the sequence shown in Fig. 5. This is clear from the determination of the first seven N-terminal amino acids of the purified protein. The *treC* gene ends with the TAA stop codon at position 3527, which is followed by a potential transcriptional termination site as indicated in the sequence (Fig. 5). Thus, *treC* encodes a protein containing 552 amino acids with a calculated molecular weight of 63,781. Upstream of *treC* we could identify a potential ribosomal binding site for *treC* and an adjacent open reading frame that continues up to the *Eco*RI site, the beginning of the sequence. This open reading frame represents the 3′ portion of the *treB* gene, whose sequence, including the transcriptional start site of the *treB-treC* operon, will be published elsewhere.

Figure 6 shows the comparison of the deduced amino acid sequence of TreC with a number of protein sequences found to be homologous by searching the protein data bank. As can be seen, TreC is homologous over the entire sequence, excluding the very C terminus, with oligo-1,6-glucosidases (sucrase-isomaltases) of *Bacillus thermoglucosidiasus* (51% identity), *B. cereus* (48% identity), and a *Bacillus* sp. (45% identity) and with dextran glucosidase of *Streptococcus equisimilis* (45% identity).

Involvement of glucokinase in trehalose metabolism. In order to estimate the contributions of glucose and glucose 6-phosphate, the products liberated by TreC, for growth on trehalose, we tested strain CB17. This strain is defective in *glk*, which encodes glucokinase; in *treA*, which encodes the periplasmic trehalase; and in *ptsG* and *ptsM*, which encode the enzyme IIs of the PTS-mediated transport systems for glucose. Thus, this strain is unable to grow on glucose. It has been observed that this strain also is unable to grow on maltose (12). We observed the same phenomenon with trehalose as the substrate. The strain cannot grow on trehalose even though it is fully active in trehalose transport (data not shown). This is surprising, since the TreC enzyme is also fully active (Table 2). As shown in Table 4, 10 mM trehalose given to cells of strain CB17 grown to stationary phase was taken up and hydrolyzed, and half of the glucose contained in trehalose was secreted into the medium. The rate of glucose formation was about 1.5 nmol of trehalose hydrolyzed per min per 10^9 cells. Growth can be restored by the introduction of either glucokinase (phosphorylating internal glucose) or enzyme EII^{Glc} (phosphorylating incoming glucose). Since the second product of TreC-mediated hydrolysis of trehalose-6-phosphate is glucose 6-phosphate, the strain should grow on trehalose even though it could use only half of its glucose content. The assumption that CB17 can use internal glucose 6-phosphate is borne out by the observation that it can grow on this compound as the sole source of carbon. CB17 is also unable to grow on galactose, even though it can grow on glycerol.

DISCUSSION

In this paper, we describe the cloning and sequencing of *treC* as well as the purification and characterization of its gene product, the trehalose-6-phosphate hydrolase of *E. coli*. To our

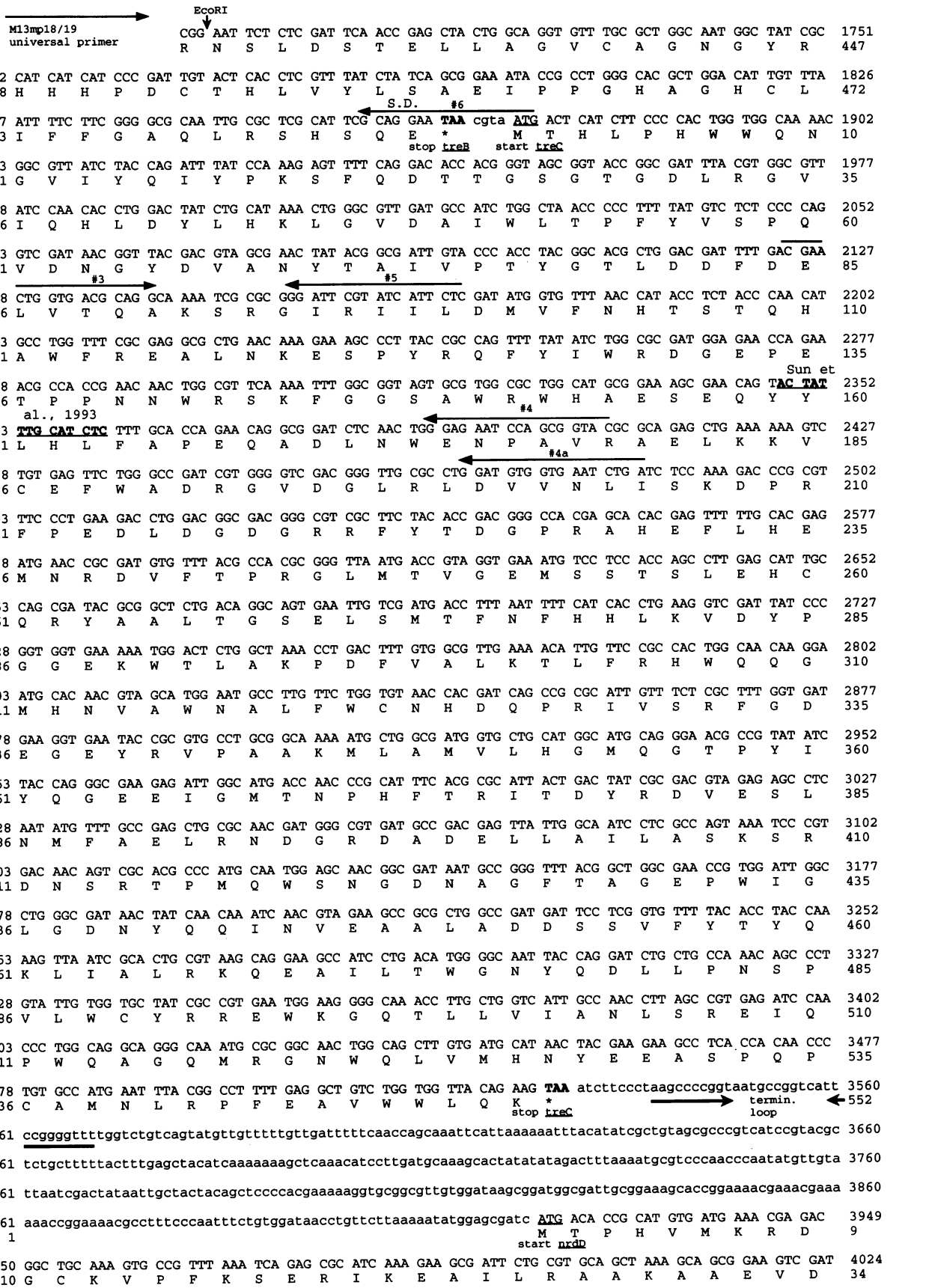
EcoRI
M13mp18/19
universal primer
S.D.
#6
stop treB
start treC
#3
#5
Sun et
al., 1993
#4
#4a
stop treC
termin.
loop
start nrdD

knowledge, this is the first time a trehalose-6-phosphate hydrolase from any organism has been cloned, purified to homogeneity, and sequenced.

treC is located immediately upstream of *nrdD*, which encodes the anaerobic ribonucleotide reductase at 96.5 min on the genetic map of *E. coli* (49). It is separated from *nrdD* by a putative transcriptional termination site (Fig. 5) followed by a promoter for *nrdD* (49). Upstream of *treC* and immediately adjacent to it is *treB*, encoding EII^{Tre}. As will be described in detail elsewhere, *treB* and *treC* form an operon (27a). Consistent with this interpretation is the observation that plasmid pUE1 (containing *treB* as well as *treC*) exhibits inducible TreC activity, whereas pRIM1 (containing *treC* and only 200 bp of the 3′ portion of *treB*) exhibits low but constitutive levels of TreC because it does not contain the main promoter of the operon. It is not clear yet whether there exists a weak promoter within the *treB* gene that allows trehalose-independent expression of *treC*. We had observed that our largest plasmid, pUE1, exhibited trehalose-inducible TreC activity that was less than the chromosomally encoded TreC activity of a wild-type strain. Preliminary results have shown that this plasmid contains upstream of the *treB-treC* operon the gene encoding the repressor for the operon. This repressor might be responsible for the lower level of expression of the pUE1-encoded *treC*.

The purified TreC protein hydrolyzed PNG but not trehalose. This prompted us to reevaluate the role and enzymatic function of TreC. It occurred to us that the *p*-nitrophenyl ring in PNG vaguely resembles the glucose 6-phosphate portion of trehalose-6-phosphate. Since this compound has now become commercially available, we could demonstrate that TreC was indeed able to hydrolyze trehalose-6-phosphate. Thus, it became clear that TreC was not an amylotrehalase, as proposed earlier (7), but a trehalose-6-phosphate hydrolase. The rate of TreC-mediated trehalose-6-phosphate hydrolysis in extracts of fully induced strains was high enough to account for the metabolic flow necessary for growth.

The rate of transport of a particular carbon source is usually considered the rate-limiting step in the degradation of the carbon source (33). In the case of trehalose metabolism, the key reaction is the hydrolysis of trehalose-6-phosphate after the PTS-mediated uptake of trehalose as trehalose-6-phosphate. Crude extracts of a fully induced wild-type strain contained an activity of 0.8 μmol of trehalose-6-phosphate hydrolyzed per min and mg of protein. With the approximation that 10^9 cells correspond to about 0.1 mg of protein (38), the V_{max} of TreC activity contained in 10^9 cells corresponds to about 80 nmol of trehalose-6-phosphate hydrolyzed per min. This value should be compared with 9 nmol/min and 10^9 cells at room temperature, the V_{max} of trehalose uptake of fully induced cells as determined by transport assays (1). On the basis of Michaelis-Menten kinetics and using a K_m of 6 mM for the enzyme and assuming the absence of any other trehalose-6-phosphate-degrading enzyme (for example, OtsB), the equilibrium concentration of intracellular trehalose-6-phosphate during growth on unlimited amounts of trehalose should therefore be about 0.76 mM. Thus, the activity of OtsB that eliminates trehalose-6-phosphate nonproductively (forming nonmetabolizable internal trehalose) will greatly affect growth on trehalose. We have demonstrated previously that the high activity of this enzyme under high-osmolarity growth conditions is responsible for the reduction of *treB-treC* expression at high osmolarity because of the lack of induction of *treB-treC* by internal trehalose-6-phosphate (28).

In order to compare TreC with other enzymes, we searched the BLAST facility of NCBI. The highest degree of homology of the deduced amino acid sequence of TreC to proteins in the data bank was to oligo-1,6-glucosidases (sucrase-isomaltases) from *Bacillus* species over the entire sequence (Fig. 6). His-105, Asp-200, Glu-250, His-324, and Asp-325 of TreC can be considered conserved amino acids in comparison with analogous sites in oligo-1,6-glucosidases of *B. cereus* (53), *B. thermoglucosidiasus* (52), and dextran glucosidase of *S. equisimilis* (37), as shown in Fig. 6. Watanabe et al. (52) compared the oligo-1,6-glucosidase sequences of *B. cereus* and *B. thermoglucosidiasus* with the sequences of *Aspergillus oryzae* α-amylase (35) and porcine pancreas α-amylase (13), both of which had been crystallized and had had their X-ray structures determined. Although the amino acid sequences of the oligo-1,6-glucosidases and the α-amylases diverged, Watanabe et al. found a strong similarity between the protein conformation of the oligo-1,6-glucosidases, predicted by the primary structure, and the known structure of the α-amylases. From this comparison, Watanabe et al. could infer which amino acids are important for the function of the active site of the glucosidases. Exactly the same amino acids (His-105, Asp-200, Glu-250, His-324, and Asp-325 of TreC) are highly conserved in TreC (Fig. 6). Watanabe et al. (52) discuss these sites as taking part in binding the α-glucosyl group of PNG or the nonreducing α-glucosyl group of isomaltosaccharide, since these terminal glucose residues are released from the corresponding substrate upon hydrolysis. Possibly, these sites in TreC have similar functions with trehalose-6-phosphate as the substrate.

The conserved Pro-18, Pro-54, Pro-59, and Pro-138 residues of TreC can be discussed in the same way, in respect to the analogous sites in *B. cereus* and *B. thermoglucosidiasus*. Watanabe et al. (52) see these proline residues as important for the conformational integrity of the active site cleft of the oligo-1,6-glucosidases compared with the α-amylase of *A. oryzae* (35).

The functions of the prominent homologous stretch of 11 identical amino acids beginning at position 360 of TreC (Fig. 6) and of 6 identical amino acids beginning at position 414 of TreC are unknown.

It seems surprising that TreC (which recognizes a sugar-phosphate) contains homology to the stretch in oligo-1,6-glucosidases (which recognize unphosphorylated sugars) which has been proposed as the active site. However, this is not without precedence, since the active sites of triose-phosphate isomerase, pyruvate kinase, and aldolase (the substrates of which are all organic phosphates) show homology to sequences proposed to form the active site in *A. oryzae* α-amylase (an enzyme recognizing unphosphorylated sugars) (35).

We did not find significant homology to enzymes hydrolyzing sucrose 6-phosphate of gram-negative bacteria that are part of the sucrose degradative pathway and genetically connected to the PTS-mediated uptake of sucrose as sucrose 6-phosphate (44). This is even more surprising, since TreB (the enzyme EII^{Tre}) is highly homologous to several sucrose PTS EII proteins (27a).

Maréchal (34) had reported earlier that *E. coli* contained a

FIG. 5. DNA sequence of *treC*. The 3′ end of *treB* and the sequence of *treC* are shown. The beginning of the sequence published by Sun et al. (49) is indicated (boldface and underlined), beginning at position 2348. Arrows above the DNA sequences indicate the primer sequences used (primers 3 to 6). The putative Shine Dalgarno sequence (S.D.) is indicated. *treC* starts with the ATG codon at position 1873. The stop codons of *treB* and *treC* (asterisks) and the putative termination loop for *treC* translation (arrows beginning at bp 3538) are shown.

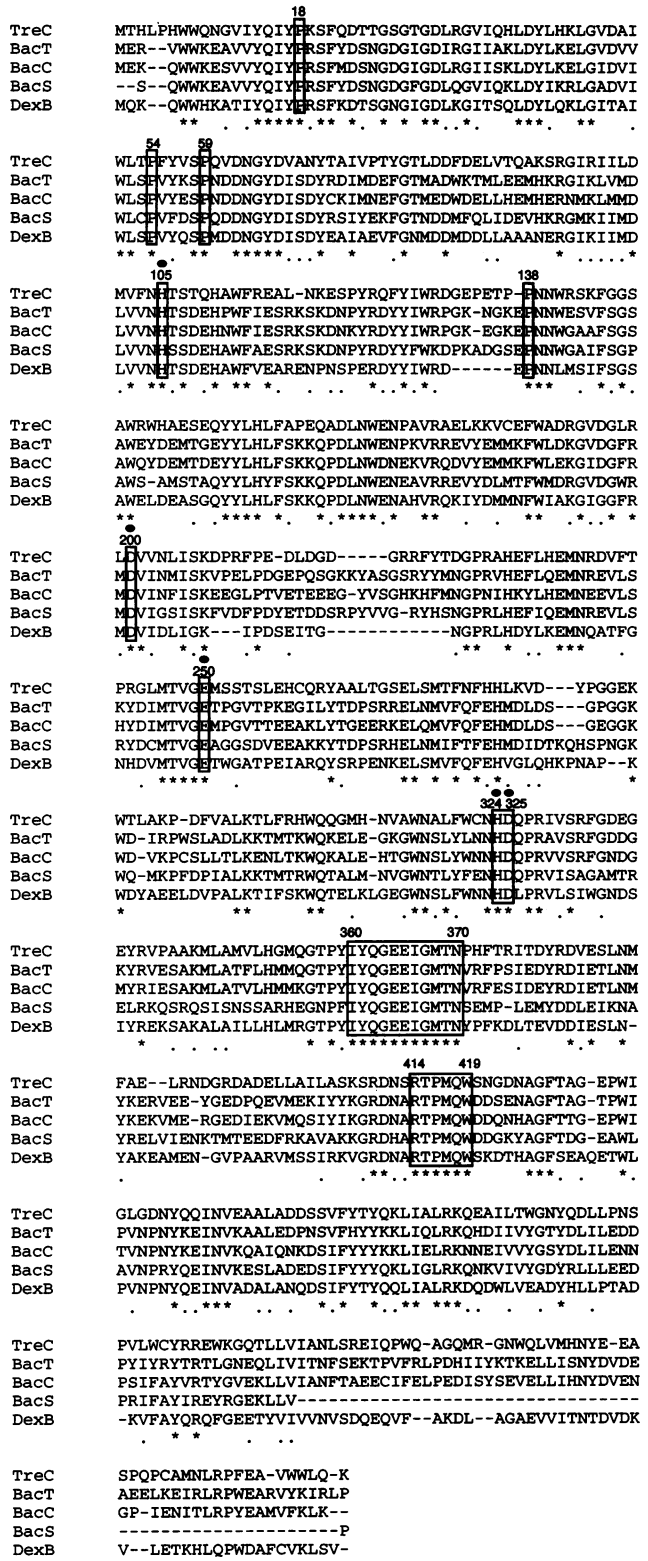

FIG. 6. Homology of TreC to oligo-1,6-glucosidases. The deduced protein sequence of TreC was analyzed in the BLAST data bank and with the ClustalV program (27). The sequences of trehalose-6-phosphate hydrolase of *E. coli* (TreC); oligo-1,6-glucosidases of *B. thermoglucosidiasus* (BacT), *B. cereus* (BacC), and a *Bacillus* sp. (BacS); and dextran glucosidase of *S. equisimilis* (DexB) are shown. Asterisks indicate identical amino acids, while dots indicate conserved amino acids. Dashes mark sites of missing amino acids. Prolines at sites 18, 54, 59, and 138 are boxed. His-105, Asp-200, Glu-250, His-324, and Asp-325 are boxed and marked with a point, indicating their possible function as part of the active site of the enzymes. The long stretches of identical amino acids (whose significance is not yet known) from positions 360 to 370 and from positions 414 to 419 in the C-terminal part of these enzymes are boxed.

TABLE 4. Formation and secretion of glucose after the uptake of trehalose by strain CB17[a]

Time (h)	mM glucose released into the medium
0	0.8
1	3.2
2	5.0
3	6.8
4.5	9.0
5	9.5
6	9.2
7	10.5
8	9.4
25	8.3

[a] CB17 cells were induced with trehalose and were concentrated to an optical density at 578 nm of 40 in MMA. Trehalose (10 mM final concentration) was added. At the indicated times, 20 μl of cells was centrifuged and the supernatant was tested for glucose content.

trehalose-6-phosphate hydrolase as well as an EII enzyme of the PTS specific for trehalose. At the time, we could not reproduce Maréchal's finding of a trehalose-6-phosphate hydrolase. Instead, the incubation of trehalose-6-phosphate with cellular extracts always yielded trehalose and some glucose, indicative for a catabolic trehalose-6-phosphate phosphatase as the first degradative enzyme (7). In retrospect, we presume that there existed in our extracts a considerable amount of trehalose-6-phosphate phosphatase, the product of *otsB*, that efficiently competed with trehalose-6-phosphate hydrolase (TreC) and produced free trehalose from this compound. As we now know, OtsB is induced not only under conditions of high osmolarity but also under stationary-growth conditions, both phenomena being dependent on the alternate sigma factor RpoS (26). The most reasonable explanation for the different results in our assays and the assays that Maréchal performed (34) is therefore that the strain Maréchal used for testing cellular extracts was grown to mid-log phase, a condition under which expression of RpoS is reduced (31), whereas we used extracts of stationary-phase cells. Thus, the extracts that Maréchal used may not have contained trehalose-6-phosphate phosphatase whereas ours did.

From this consideration and as already mentioned above, it appears that trehalose-6-phosphate phosphatase, the *otsB* gene product, is critical for the ability of the cell to metabolize trehalose. It seems that OtsB, the trehalose-6-phosphate phosphatase (in the absence of TreA, the periplasmic trehalase), curtails growth on trehalose, particularly when stationary-phase cells are inoculated in trehalose-containing media. Long lag phases are notorious in studies of growth on trehalose (30).

Another interesting phenomenon is the observation that a *treA ptsM ptsG glk* strain which lacks any enzymatic activity to phosphorylate glucose is unable to grow on trehalose even though it is fully active in uptake of trehalose as trehalose-6-phosphate and in its hydrolysis to glucose and glucose 6-phosphate. Despite the fact that these cells lack their glucose

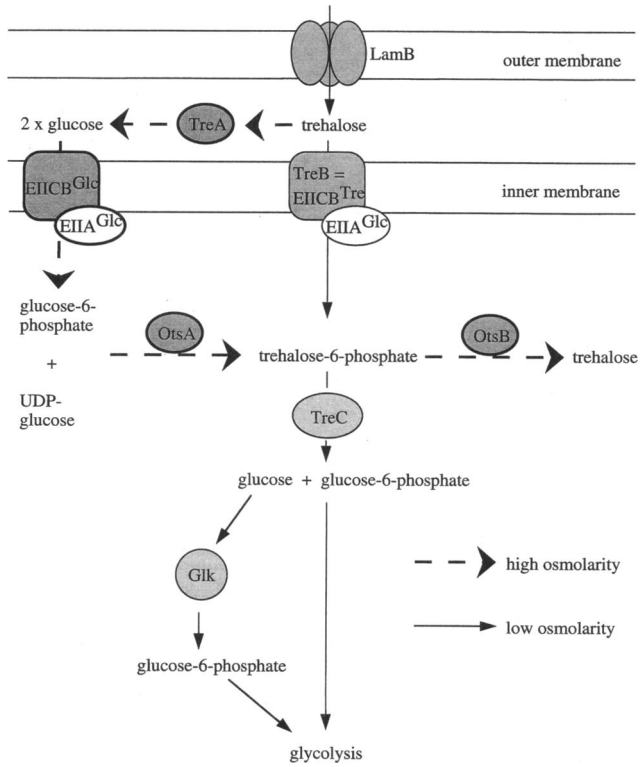

FIG. 7. Model of trehalose metabolism in *E. coli*. Trehalose diffuses into the periplasm through the LamB pore (LamB). Under low-osmolarity conditions, trehalose is transported into the cell under simultaneous phosphorylation by enzyme EIICB^{Tre} (TreB) of the PTS, using EIIA of the glucose PTS (EIIA^{Glc}) as the phosphoryl donor. Internally, trehalose-6-phosphate is hydrolyzed to glucose and glucose 6-phosphate by the trehalose-6-phosphate hydrolase (TreC). Free glucose is phosphorylated by glucokinase (Glk), and glucose 6-phosphate undergoes glycolysis. At high osmolarity, TreB and TreC are repressed. Trehalose is hydrolyzed in the periplasm to two molecules of glucose by the periplasmic trehalase (TreA). Glucose is then transported into the cells by the glucose PTS. On the other hand, trehalose is synthesized under high-osmolarity conditions by the trehalose-6-phosphate synthase (OtsA) and the trehalose-6-phosphate phosphatase (OtsB), using glucose 6-phosphate and UDP-glucose as substrates.

transport systems, they effectively excrete the unusable glucose through an as-yet-unknown pathway (Table 4). It is unclear why the retained glucose 6-phosphate is not able to support growth. The same phenomenon can be observed with the utilization of maltose in a very similar strain. In this case, unusable glucose is also secreted and the remaining maltodextrins cannot support growth despite the presence of maltodextrin phosphorylase (12). It seems that for growth on glycolytic carbon sources, the cell needs the capacity to phosphorylate glucose, indicating at the same time the presence of a cytoplasmic activity hydrolyzing glucose 6-phosphate or glucose 1-phosphate to glucose (19).

Figure 7 represents our present view of trehalose metabolism in *E. coli*. At high osmolarity, OtsA and OtsB are present at high levels and synthesize internal trehalose from UDP-glucose and glucose 6-phosphate (46). At the same time, the TreB-mediated uptake of trehalose as trehalose-6-phosphate and its TreC-mediated hydrolysis to glucose and glucose 6-phosphate are prevented by the OtsB-mediated removal of internal trehalose-6-phosphate, this compound being the inducer of the *treB-treC* operon (28) as well as the substrate of the TreC protein. Nevertheless, the utilization of exogenous trehalose as a carbon source is still possible at high osmolarity because of the hydrolysis of trehalose to glucose in the periplasm by the osmotically-inducible periplasmic trehalase (TreA), followed by the PTS-mediated uptake of glucose as glucose 6-phosphate.

At low osmolarity, provided that the level of OtsB is low, trehalose is taken up by TreB as trehalose-6-phosphate and hydrolyzed by TreC to glucose and glucose 6-phosphate, which are then subjected to glucose phosphorylation to glucose 6-phosphate and glycolysis.

Future studies will have to concentrate on the regulatory role of OtsB in the utilization of internal trehalose-6-phosphate as well as on the role of internal-glucose phosphorylation. The latter aspect is important for the utilization of not only trehalose but also other disaccharides, such as maltose and lactose, as well as the monosaccharide galactose.

ACKNOWLEDGMENTS

We thank Wolfgang Klein for making subclones in M13 available to us and for helpful discussions. We thank Petra Dersch for plasmid pPD1, I. Rasched for performing the N-terminal amino acid sequencing of TreC, and X. Sun and B.-M. Sjöberg for sending sequences. Jan Lucht and Kenn Rudd were very helpful in handling our sequence data.

Financial support was obtained from the Deutsche Forschungsgemeinschaft (SFB156) and the Fond der Chemischen Industrie. M.R. was the recipient of a fellowship of the Studienstiftung des deutschen Volkes.

REFERENCES

1. **Altschul, S. F., W. Gish, W. Miller, E. W. Myers, and D. J. Lipman.** 1990. Basic local alignment search tool. J. Mol. Biol. **215:**403–410.
2. **Barham, D., and P. Trinder.** 1972. An improved colour reagent for the determination of blood glucose by the oxidase system. Analyst **97:**142–145.
3. **Biggin, M. D., T. J. Gibson, and G. F. Houg.** 1983. Buffer gradient gels and ^{35}S-label as an aid to rapid DNA sequence determination. Proc. Natl. Acad. Sci. USA **80:**3963–3965.
4. **Bochner, B. R., H. Huang, G. L. Schieven, and B. N. Ames.** 1980. Positive selection for loss of tetracycline resistance. J. Bacteriol. **143:**926–933.
5. **Bolivar, F., R. L. Rodriguez, P. J. Greene, M. C. Betlach, H. L. Heyneker, and H. W. Boyer.** 1977. Construction and characterization of new cloning vehicles. II. A multipurpose cloning system. Gene **2:**95–113.
6. **Boos, W., U. Ehmann, E. Bremer, A. Middendorf, and P. Postma.** 1987. Trehalase of *Escherichia coli*. Mapping and cloning of its structural gene and identification of the enzyme as a periplasmic protein induced under high osmolarity growth conditions. J. Biol. Chem. **262:**13212–13218.
7. **Boos, W., U. Ehmann, H. Forkl, W. Klein, M. Rimmele, and P. Postma.** 1990. Trehalose transport and metabolism in *Escherichia coli*. J. Bacteriol. **172:**3450–3461.
8. **Booth, I. R., J. Cairney, L. Sutherland, and C. F. Higgins.** 1988. Enteric bacteria and osmotic stress: an integrated homeostatic system. J. Appl. Bacteriol. Symp. Suppl., p. 35S–49S.
9. **Bradford, M. M.** 1976. A rapid and sensitive method for the quantitation of microgram quantities of protein utilizing the principle of protein-dye binding. Anal. Biochem. **72:**248–254.
10. **Brand, B., and W. Boos.** 1989. Convenient preparative synthesis of [^{14}C]trehalose from [^{14}C]glucose by intact *Escherichia coli* cells. Appl. Environ. Microbiol. **55:**2414–2415.
11. **Britten, R. J., and F. T. McClure.** 1962. The amino acid pool in *Escherichia coli*. Bacteriol. Rev. **26:**292–335.
12. **Buhr, A., G. A. Daniels, and B. Erni.** 1992. The glucose transporter of *Escherichia coli*. Mutants with impaired translocation activity that retain phosphorylation activity. J. Biol. Chem. **267:**3847–3851.
13. **Buisson, G., E. Duée, R. Haser, and F. Payan.** 1987. Three

dimensional structure of porcine pancreatic α-amylase at 2.9 Å resolution. Role of calcium in structure and activity. EMBO J. **13**:3909–3916.
14. **Casadaban, M. J.** 1976. Transposition and fusion of the *lac* genes to selected promoters in *Escherichia coli* using bacteriophage lambda and Mu. J. Mol. Biol. **104**:541–555.
15. **Chen, Y.-M., Y. Zhu, and E. C. C. Lin.** 1987. The organization of the *fuc* regulon specifying L-fucose dissimilation in *Escherichia coli* K-12 as determined by gene cloning. Mol. Gen. Genet. **210**:331–337.
16. **Crowe, J. H., L. M. Crowe, J. F. Carpenter, A. S. Rudolph, C. Aurell Wistrom, B. J. Spargo, and T. J. Anchordoguy.** 1988. Interactions of sugars with membranes. Biochim. Biophys. Acta Biomembr. Rev. **947**:367–384.
17. **Crowe, J. H., L. M. Crowe, and D. Chapman.** 1984. Preservation of membranes in anhydrobiotic organisms: the role of trehalose. Science **223**:701–703.
18. **Curtis, S. J., and W. Epstein.** 1975. Phosphorylation of D-glucose in *Escherichia coli* mutants defective in glucosephosphotransferase, mannosephosphotransferase, and glucokinase. J. Bacteriol. **122**:1189–1199.
19. **Decker, K., R. Peist, J. Reidl, M. Kossmann, B. Brand, and W. Boos.** 1993. Maltose and maltotriose can be formed endogenously in *Escherichia coli* from glucose and glucose-1-phosphate independently of enzymes of the maltose system. J. Bacteriol. **175**:5655–5665.
20. **Dersch, P., K. Schmidt, and E. Bremer.** 1993. Synthesis of the *Escherichia coli* K-12 nucleoid-associated DNA-binding protein H-NS is subjected to growth phase control and autoregulation. Mol. Microbiol. **8**:875–889.
21. **Dinnbier, U., E. Limpinsel, R. Schmid, and E. P. Bakker.** 1988. Transient accumulation of potassium glutamate and its replacement by trehalose during adaptation of growing cells of *Escherichia coli* K12 to elevated sodium chloride concentrations. Arch. Microbiol. **150**:348–357.
22. **Freundlieb, S., and W. Boos.** 1986. α-Amylase of *Escherichia coli*, mapping and cloning of the structural gene, *malS*, and identification of its product as a periplasmic protein. J. Biol. Chem. **261**:2946–2953.
23. **Giæver, H. M., O. B. Styrvold, I. Kaasen, and A. R. Strøm.** 1988. Biochemical and genetic characterization of osmoregulatory trehalose synthesis in *Escherichia coli*. J. Bacteriol. **170**:2841–2849.
24. **Gutierrez, C., M. Ardourel, E. Bremer, A. Middendorf, W. Boos, and U. Ehmann.** 1989. Analysis and DNA sequence of the osmoregulated *treA* gene encoding the periplasmic trehalase of *Escherichia coli* K12. Mol. Gen. Genet. **217**:347–354.
25. **Hazelbauer, G. L.** 1975. The maltose chemoreceptor of *Escherichia coli*. J. Bacteriol. **122**:206–214.
26. **Hengge-Aronis, R., W. Klein, R. Lange, M. Rimmele, and W. Boos.** 1991. Trehalose synthesis genes are controlled by the putative sigma factor encoded by *rpoS* and are involved in stationary-phase thermotolerance in *Escherichia coli*. J. Bacteriol. **173**:7918–7924.
27. **Higgins, D. G., A. J. Bleasby, and R. Fuchs.** 1992. ClustalV: improved software for multiple sequence alignment. Cabios **8**:189–191.
27a. **Klein, W., and W. Boos.** Unpublished results.
28. **Klein, W., U. Ehmann, and W. Boos.** 1991. The repression of trehalose transport and metabolism in *Escherichia coli* by high osmolarity is mediated by trehalose-6-phosphate phosphatase. Res. Microbiol. **142**:359–371.
29. **Laemmli, U. K.** 1970. Cleavage of structural proteins during the assembly of the head of bacteriophage T4. Nature (London) **227**:680–685.
30. **Lang, H. N., and E. T. Palva.** 1993. The *ompS* gene of *Vibrio cholerae* encodes a growth phase-dependent maltoporin. Mol. Microbiol. **10**:891–901.
31. **Lange, R., and R. Hengge-Aronis.** 1994. The cellular concentration of the σ^s subunit of RNA polymerase in *Escherichia coli* is controlled on the levels of transcription, translation and protein stability. Genes Dev. **8**:1600–1612.
32. **Larsen, P. I., L. K. Sydnes, B. Landfald, and A. R. Strøm.** 1987. Osmoregulation in *Escherichia coli* by accumulation of organic osmolytes: betaines, glutamic acid, and trehalose. Arch. Microbiol. **147**:1–7.
33. **Lengeler, J. W.** 1993. Carbohydrate transport in bacteria under environmental conditions, a black box? Antonie van Leeuwenhoek Int. J. Gen. Mol. Microbiol. **63**:275–288.
34. **Maréchal, L. R.** 1984. Transport and metabolism of trehalose in *Escherichia coli* and *Salmonella typhimurium*. Arch. Microbiol. **137**:70–73.
35. **Matsuura, Y., M. Kusunoki, W. Harado, and M. Kakudo.** 1984. Structure and possible catalytic residues of Taka-amylase A. J. Biochem. **95**:697–702.
36. **May, G., E. Faatz, M. Villarejo, and E. Bremer.** 1986. Binding protein-dependent transport of glycine betaine and its osmotic regulation in *Escherichia coli* K12. Mol. Gen. Genet. **205**:225–233.
37. **Mechold, U., K. Steiner, S. Vettermann, and H. Malke.** 1993. Genetic organization of the streptokinase region of the *Streptococcus equisimilis* H46A chromosome. Mol. Gen. Genet. **241**:129–140.
38. **Miller, J. H.** 1972. Experiments in molecular genetics. Cold Spring Harbor Laboratory Press, Cold Spring Harbor, N.Y.
39. **Norrander, J., T. Kempe, and J. Messing.** 1983. Construction of improved M13 vectors using oligodeoxynucleotide-directed mutagenesis. Gene **26**:101–106.
40. **Pugsley, A. P., and C. Dubreuil.** 1988. Molecular characterization of *malQ*, the structural gene for the *Escherichia coli* enzyme amylomaltase. Mol. Microbiol. **2**:473–479.
41. **Reeve, J.** 1979. Use of minicells for bacteriophage-directed polypeptide synthesis. Methods Enzymol. **68**:493–503.
42. **Sambrook, J., E. F. Fritsch, and T. Maniatis.** 1989. Molecular cloning: a laboratory manual, 2nd ed. Cold Spring Harbor Laboratory Press, Cold Spring Harbor, N.Y.
43. **Sanger, F., S. Nicklen, and A. R. Coulson.** 1977. DNA sequencing with chain-terminating inhibitors. Proc. Natl. Acad. Sci. USA **74**:5463–5467.
44. **Schmid, K., R. Ebner, K. Jahreis, J. W. Lengeler, and F. Titgemeyer.** 1991. A sugar-specific porin, *scrY*, is involved in sucrose uptake in enteric bacteria. Mol. Microbiol. **5**:941–950.
45. **Strøm, A. R., P. Falkenberg, and B. Landfald.** 1986. Genetics of osmoregulation in *Escherichia coli*: uptake and biosynthesis of organic osmolytes. FEMS Microbiol. Rev. **39**:79–86.
46. **Strøm, A. R., and I. Kaasen.** 1993. Trehalose metabolism in *Escherichia coli*, stress protection and stress regulation of gene expression. Mol. Microbiol. **8**:205–210.
47. **Studier, F. W., and B. A. Moffat.** 1986. Use of bacteriophage T7 RNA polymerase to direct selective high-level expression of cloned genes. Mol. Biol. **189**:113–130.
48. **Styrvold, O. B., and A. R. Strøm.** 1991. Synthesis, accumulation, and excretion of trehalose in osmotically stressed *Escherichia coli* K-12 strains: influence of amber suppressors and function of the periplasmic trehalase. J. Bacteriol. **173**:1187–1192.
49. **Sun, X., J. Harder, M. Krook, H. Jörnvall, B.-M. Sjöberg, and P. Reichard.** 1993. A possible glycine radical in anaerobic ribonucleotide reductase from *Escherichia coli*: nucleotide sequence of the cloned *nrdD* gene. Proc. Natl. Acad. Sci. USA **90**:577–581.
50. **Tabor, S., and C. C. Richardson.** 1985. A bacteriophage T7 RNA polymerase/promoter system for controlled exclusive expression of specific genes. Proc. Natl. Acad. Sci. USA **82**:1074–1078.
51. **Takeshita, S., M. Sato, M. Toba, W. Masahashi, and T. Hashimoto-Gotoh.** 1987. High-copy-number and low-copy-number plasmid vectors for *lacZ* α-complementation and chloramphenicol- or kanamycin-resistance selection. Gene **61**:63–74.
52. **Watanabe, K., K. Chishiro, K. Kitamura, and Y. Suzuki.** 1991. Proline residues responsible for thermostability occur with high frequency in the loop regions of an extremely thermostable oligo-1,6-glucosidase from *Bacillus thermoglucosidiasus* KP1006. J. Biol. Chem. **266**:24287–24294.
53. **Watanabe, M., K. Kitamura, H. Iha, and Y. Suzuki.** 1990. Primary structure of the oligo-1,6-glucosidase of *Bacillus cereus* ATCC7064 deduced from the nucleotide sequence of the cloned gene. Biochemistry **192**:609–620.
54. **Wiesmeyer, H., and M. Cohn.** 1960. The characterization of the pathway of maltose utilization by *Escherichia coli*. II. General properties and mechanism of action of amylomaltase. Biochim. Biophys. Acta **39**:427–439.
55. **Yanisch-Perron, C., J. Vieira, and J. Messing.** 1985. Improved M13 phage cloning vectors and host strains: nucleotide sequences of the M13mp18 and pUC19 vectors. Gene **33**:103–119.